2019 IEEE World Haptics Conference (WHC)
Tokyo, Japan
9-12 July 2019

Stiction rendering in touch

Roman V. Grigorii Michael A. Peshkin J. Edward Colgate

Abstract— **Human perception of surface stickiness is closely related to intermittent slip dynamics, or stiction. In this work, we develop a method for real-time closed-loop rendering of surface stiction on an electroadhesive surface haptic display, and test it on a custom-built tribometer. We perform a psychophysical study to determine the effectiveness of a single, user-adjustable parameter on perceived surface stickiness, and elucidate what aspect of friction shapes the percept.**

I. Introduction

Dynamic skin deformation on a human hand contains rich information about the object it is interacting with [1]. Slip direction, surface profile, and overall forces on the skin contact patch can be neurally encoded and serve several key functions such as forming a body of control inputs for anticipatory actions during object grasping [2], [3]. The significance of these cues can be appreciated by observing that object manipulation becomes considerably hindered when cutaneous mechanoreceptors are anesthetically muted to excitation [4], [5]. In the context of surface texture, shear forces acting on the skin and the resulting vibrations provide information by which textures can be classified [6], [7]. Moreover, considerable evidence suggests that differences in skin vibrations elicited during touch are responsible for much of the perceptual difference among textures [8]. Across a range of tasks and conditions of touch, skin excitation serves as a mechanism to reliably quantify the characteristics of the physical world.

The complexity of texture perception has forced most studies to be narrow in scope. For instance in experiments, the finger is usually stimulated by traversal of a texture at a fixed velocity, normal load, and angle of finger incidence. This constrained experimental technique doesn't fully reflect the nature of free surface exploration. In addition, although attempts are typically made to keep the range of kinematic parameters diverse, some dynamic states of the finger in relation to the surface are often overlooked. Among these is the transient state of the finger patch that occurs during onset of finger motion such as swipe initiation or a reversal in direction. Some evidence suggests that cues generated in this time window, which corresponds to partial slip of the finger, are crucial for object manipulation [5], [9]. However, while the dynamics of the finger patch during slip onset have been well characterized [10], [11], only limited work has addressed the significance of the associated cues with the perception of surface qualities [12]. In this paper we contribute to this line of research by investigating the role that partial slip plays in forming an impression of surface stickiness. Our approach employs a novel surface haptics rendering method in which friction is varied in real time as closed-loop function of measured forces.

Surface haptic rendering techniques have generally been limited to open-loop control where the finger is assumed to be in a fully dynamic state. A more complete method, which handles the partial slip state of the finger, has yet to be presented. One of the difficulties in developing a closed-loop friction control scheme is that the friction forces may vary drastically over the course of contact time due to effects of skin viscoelasticity and occlusion [13]. In addition, friction is sensitive to contact conditions controlled by the user, such as loading forces and scan velocity [13]. With these limitations in mind, we don't make it our goal to achieve full control of the friction experienced during touch. Instead, we seek to exploit electroadhesion to modulate the partial slip phenomenon. Specifically, the control scheme presented in this paper provides the user control over the friction force necessary for the finger patch to transition from stuck to a full slip state. We find that this method of finger-pad actuation serves as a robust approach to rendering "stickiness" of the haptic surface.

II. Background

A. Electroadhesion

Ultrasonic vibration or electroadhesion can be used to modulate fingertip friction [14]–[16]. Either method can be used to produce surface haptic effects, and they can also be combined for increased friction range [17]. One of the drawbacks of ultrasonic friction modulation, however, is that the strength of the effect tends to vary across the screen according to finger location on the vibrating substrate. Also, electroadhesion has a comparatively wider bandwidth, which allows for quick transitions in applied friction force [15]. In current work we use electroadhesion as the friction modulation approach.

Empirical evidence suggests that the friction force exerted on a human finger in contact with a flat electroadhesive surface can be modeled by [15]:

$$F = \mu_k(W + F_e) \tag{1}$$

Where μ_k is the coefficient of dynamic friction between the finger and display surface, W and F_e are normal and electroadhesion forces respectively. Electroadhesion force originates from the Coulomb attraction of the charge (free or bound) on the surfaces of the screen and finger. The electrical interaction of these two surfaces can be modeled as that of

978-1-5386-9461-9/19/$31.00 © 2019 IEEE

two oppositely charged plates of a parallel plate capacitor, and the attractive force between them is given by:

$$F_e = \frac{\epsilon A_{gross} |V_{gap}|^2}{2d^2} = \frac{\epsilon A_{gross} |I_{gap}|^2 |Z_{gap}|^2}{2d^2} \quad (2)$$

Where ϵ is permitivity of air, A_{gross} is gross contact area, I_{gap} is the current applied across the gap, d is the width of effective gap between the skin and screen, and Z_{gap} is it's electrical impedance as modeled in [18]. As the outermost layer of skin is pulled close to the display by the electric field in the gap, skin asperities are deformed creating additional contact points with the surface. Weakly interacting intermolecular bonds form at the location of intimate contact and contribute to an increase in adhesion, and therefore, friction force. The deformation of asperities which leads to increased contiguous contact can be equivalently achieved by applied normal load, hence eq. 1. The relative strength of F_e is controlled by the voltage across the gap, which is in turn set by the gap impedance and the displacement current. For a number of reasons, primary of which is safety, we use a controlled current to apply electroadhesive force.

It has been observed that the gap voltage applied at ultrasonic frequencies produces a very stable electroadhesion force compared to a gap voltage applied at DC [15]. A preliminary experiment was performed by the author, where a 8 $\mathrm{mA_{pp}}$ 20 kHz current signal was applied to effect electroadhesion. No significant variation of friction force over time that would be characteristic to mechanisms associated with build up and absorption of moisture were observed. We therefore deem the contributions of time-dependent contact conditions to variations of electroadhesive force insignificant in current work. We use a current carrier frequency of 20 kHz that we modulate according to desired strength of the effect.

B. Dynamics of slip onset

As the finger begins its motion against a flat, topographically smooth surface, the skin patch region initially in static contact begins to slip in an annular fashion [11]. Skin at the patch edge begins to slip first. The slipping area then grows inward, replacing the regions in fully static contact, as the applied shear force grows. The dynamics of finger slip gives rise to stiction, where the stiction coefficient, μ_s, is defined as the threshold value of shear to normal force ratio that must be overcome for full slip. The bulk shear force exerted on the contact patch during an onset of slip has been modeled from empirical evidence by [11]:

$$F = \tau_o A + \beta W (1 - \alpha) \quad (3)$$

Where τ_o is the interface shear component that contributes to a pressure independent component of friction and A is the real contact area. α is the ratio of patch area in static contact to the total gross area patch. β is a constant value capturing pressure sensitive contributions of the friction mechanism and is akin to μ_k in that manner. The contribution of electroadhesion to eq. 4 is expected to be equivalent to one in eq. 1, namely:

$$F = \tau_o A + \beta (W + F_e)(1 - \alpha) \quad (4)$$

The effect of electroadhesion on the intrinsic shear value, τ_o, is expected to be negligible since gap impedance tends to be shorted out during static contact. Due to lack of empirical evidence for these contentions, however, we settle only on the conclusion that the contribution of electroadhesive force is that of increasing the lateral force, F necessary to transition the finger pad from stuck to a sliding. In effect, we hope that application of electroadhesion can alter the partial slip dynamics of finger patch in a controllable fashion.

III. Methods

A. Stiction rendering approach

Over short time and length scales, the skin of human finger is elastic in nature. Therefore, an increase in shear force needed to overcome static contact results in a proportional increase in the skin stretch achieved before the contact fails. A similar mechanism is often applied in impedance based friction rendering schemes, where small displacements from the starting position of an end-effector generate a feedback force according to Hooke's law until a critical displacement is achieved [19]. This creates a convincing illusion of "stickiness" in the simulated virtual environment. The perceptual quality of such rendering shouldn't come as a surprise since a similar mechanism can exist in touch.

We target the skin transition from stuck to full slip as the window of time during which to modulate surface friction. Application of electroadhesion during this period can effectively increase the lateral force required for such a transition to occur. For a perceptually salient effect an accurate sensing of patch state is required to identify finger states and actuate the patch accordingly. While this could be accomplished with camera-based measurement of the contact patch, such a method would be limited to transparent substrates and might prove computationally expensive. We adopted the more expeditious approach of estimating contact patch state on the basis of lateral and normal force measurements.

B. Stiction algorithm

Figure 1A depicts the lateral to normal force ratio, η, as a function of swipe time as the lead author swiped his finger on the unactuated 3M glass. We separate finger patch dynamics into three presumed states: stuck, partial slip, and full slip and use η and its first derivative to identify state transitions. For instance, we assume that the state is stuck whenever $|\eta|$ is below a threshold that we call γ. γ is set to a value (e.g., 0.1) well below the kinetic friction coefficient of the touch surface. The precise value of γ is found to have minimal perceptual significance since it affects only the transition into the stuck state, not out of it.

From the stuck state, the finger can transition only into the partial slip state. This transition is indicated by a sudden reduction in $|\dot{\eta}|$ (Figure 1B, point 2) . Kinematics of surface exploration tend to contain lower frequencies ($<$10Hz) than patch dynamics ($>$100Hz) which helps to avoid confusing a

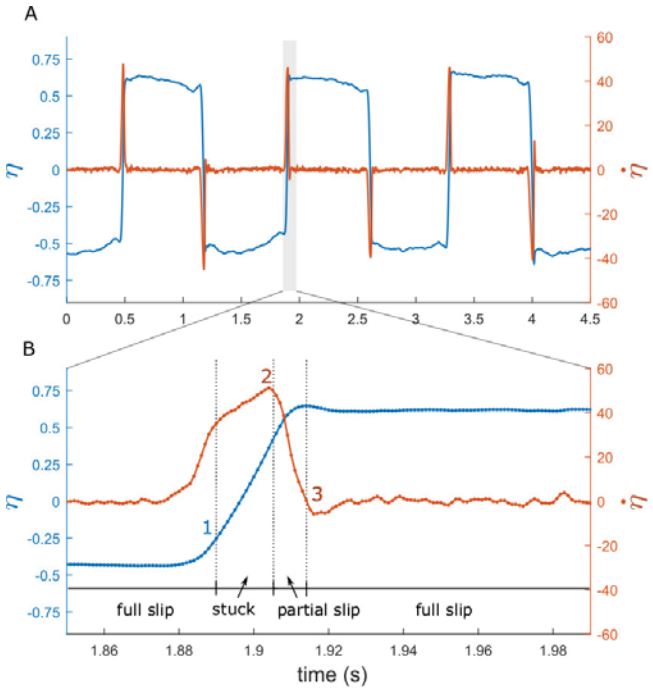

Fig. 1. A) Lateral friction to normal force ratio, η, and its time derivative, $\dot{\eta}$, sampled as the finger was moved back and forth over the unactuated electrostatic display. B) A section of graph in A (marked by a shadowed region) expanded in time. Stuck, partial slip, and full slip states of the contact patch are estimated using η and $\dot{\eta}$ values. Enumerated points indicate the time and the type of data used to locate these transitions.

sudden change in finger velocity for partial slip. While in the stuck state, the algorithm tracks the value of $|\dot{\eta}|$ and holds the maximum, $|\dot{\eta}_{max}|$. When $\frac{|\dot{\eta}|}{|\dot{\eta}_{max}|}$ falls below a threshold, δ, the state transitions from stuck to partial slip.

In principle, the transition from partial slip to full slip is quite subtle: [20] has demonstrated that, for the case $\mu_s > \mu_k$, the stuck region during partial slip may continue to shrink with increased shear but seemingly "vanish" with respect to η. Nonetheless, having only force measurements at our disposal, we assume that full slip has been reached when $|\eta|$ (Figure 1B, point 3) stops increasing. This point corresponds to the first zero crossing of $\dot{\eta}$, as shown in Figure 1.

Finally, a threshold value of applied normal load, W_{min}, is required before turning on the stickiness effect. This is necessary because the computation of η becomes unreliable at low normal force and light touch may trigger unanticipated dynamics of touch.

The stiction algorithm sets the electroadhesive current I_{out} to one of three values, each associated with a state of the contact patch: I_s (stuck), I_{ps} (partial slip), I_{fs} (full slip). Although we suspect that the stickiness information is mostly contained in the value of I_{ps}, we set I_s = I_{ps} for reasons discussed in II B. Their value constitutes the subject-adjusted parameter to modulate the perceived stickiness of the surface. I_{fs} was set to 0 throughout the experiment but can be allowed to vary. Pseudo-code for the stiction rendering algorithm is shown below, with parameter values used in the psychophysical experiment shown in parentheses:

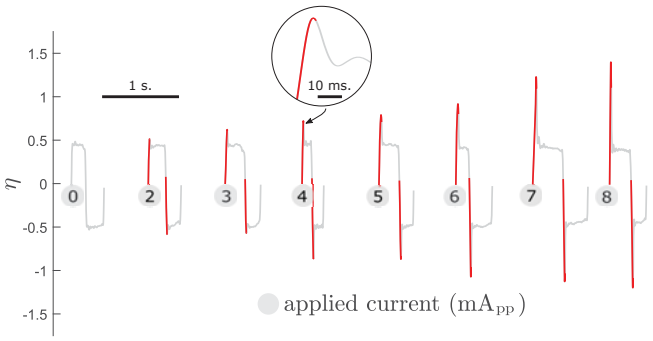

Fig. 2. Examples of rendered forces using the stiction algorithm on the lead author's hand as he freely explored the haptic surface. The grey and red curves represent the current being off and on respectively during one swipe cycle under varied applied electroadhesion current.

$I_{out} = 0$
while $W \geq W_{min}(= .025N)$ **do**
  $\eta_{old} = \eta$
  $\dot{\eta}_{old} = \dot{\eta}$
  $\eta = \frac{F}{W}$
  $\dot{\eta} = \frac{\eta - \eta_{old}}{\Delta t}$
  if $|\eta| < \gamma(= 0.1)$ **then**
    state = stuck
    $\eta_{max} = 0$
  if state is stuck **then**
    $I_{out} = I_s(varied)$
    if $|\dot{\eta}_{max}| < |\dot{\eta}|$ **then**
      $\dot{\eta}_{max} = \dot{\eta}$
    if $\frac{\dot{\eta}}{\dot{\eta}_{max}} < \delta(= .9)$ **then**
      state = partial slip
  if state is partial slip **then**
    $I_{out} = I_{ps}(varied)$
    if $\dot{\eta}_{old}\dot{\eta} \leq 0$ **then**
      state = full slip
  if state is full slip **then**
    $I_{out} = I_{fs}(= 0)$

The performance of this control scheme in action can be observed in Figure 2.

The current-controlled electrostatic display used to render stimuli for the psychophysical study is shown in Figure 3. The tactile display consisted of a 3M Microtouch SCT3250EX screen cut to 35 x 165 mm. Masking the edges containing conductive elements reduced the area accessible to touch to 28 x 160 mm. The 3M glass was mounted onto an aluminum platform supported by leaf springs compliant in the lateral direction. The platform was preloaded against a Honeywell FSS1500NSR force sensor which recorded lateral shear forces applied by the finger to the display. The leaf springs were mounted to a second platform sitting below the first. This bottom platform rested on four FSS1500NSR force sensors that were positioned below each of its corners and that were preloaded with four leaf springs compliant in the normal direction. The resulting set-up allowed for

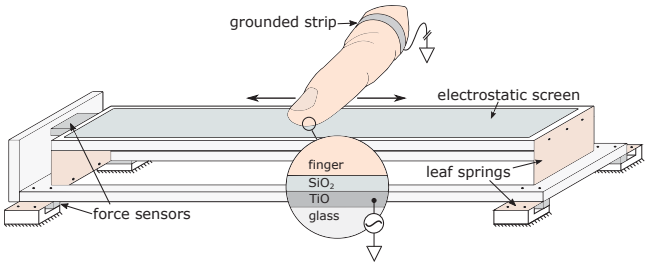

Fig. 3. Electrostatic device used in the experiment.

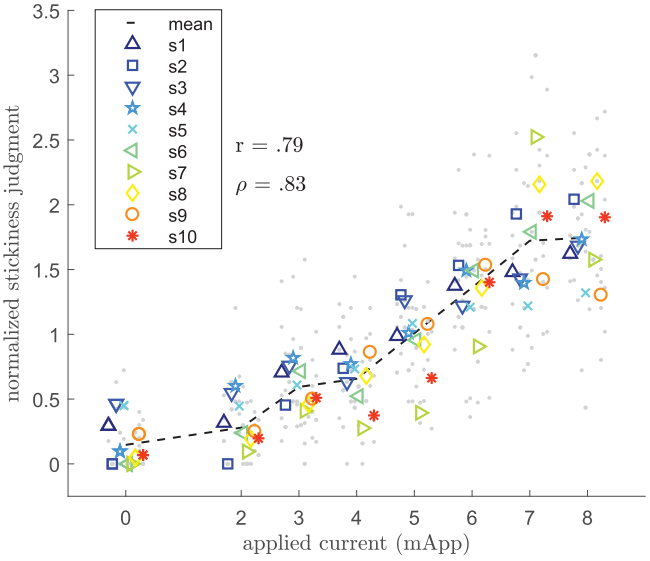

Fig. 4. Stickiness judgments normalized within each subject for eight stimuli. Outliers were removed if they were 1.5 interquartile ranges above or below upper or lower quartiles, removing less than 5% of the original data. Pearson's r and Spearman's ρ are included to show correlation strength. Grey points represent per trial subject results. Mean subject judgment is represented by colored shapes. The dashed black line represents the mean normalized judgment across all subjects. Points have been shifted about each stimulus to make the judgment of each subject more apparent.

simultaneous sensing of forces in the lateral and normal directions. The four normal force sensors were adjusted to have the same sensitivity to applied load and their readings were summed to a single normal force value. Both lateral and normal force measurements showed unloaded variance < 1 mN and force range of 0-3 N. A flat frequency response is observed for the device in DC-190 Hz range, with upper frequency cutoff marked by 6 dB gain from DC. Real-time collection and processing of the lateral and normal force data was performed by a PIC32MX795F microcontroller. The controller sampled 12 bit lateral and normal force data at 10 kHz using an external ADC. The data were low-pass filtered at 150 Hz with an IIR filter to minimize resonance contributions to force readings, and further re-sampled by averaging to 1 kHz to minimize random noise. This process offered reliable readings of force data while ensuring low response delay (< 3 ms).

C. Experimental apparatus

The microcontroller executed the stiction rendering algorithm at 1 kHz and output the modulation amplitude value. A 20 kHz carrier was created and internally modulated by a RIGOL DG1032 function generator with the modulation signal. This voltage signal was converted to current using a high-bandwidth current amplifier the characteristics of which are detailed in [15]. The modulation signal, along with lateral and normal force data, were separately recorded and retained for analyses.

D. Subject experiment

5 male and 5 female subjects aged between 22 and 31 years participated in the psychophysics study. The study was approved by the Northwestern University IRB, all subjects were financially compensated, and all subjects gave informed consent. All but one subject were right handed. Set-up adjustments were made for left handed subjects to perform the task with their dominant hand.

Prior to the experiment each subject washed his or her hands with soap and dried them with a towel. Subjects were then seated in front of the device, their dominant hand positioned on a hand rest with the index finger reaching over and touching the 3M screen positioned 1cm below the surface of the hand rest. The other hand was used to record responses on a touchscreen that was comfortably positioned on the other side of the haptic device. Pink noise was played through noise-canceling headphones for the duration of the experiment to prevent acoustic cues.

The training session, which preceded the experiment, began by asking each subject to freely explore the unactuated haptic display. When they felt familiar with the feel of the surface, the stiction effect was turned on to its maximum strength by applying a 8 $\mathrm{mA_{pp}}$ current according to the stiction algorithm. When subjects became familiar with the effect and reported feeling a difference from the unactuated display they stopped and reported on their experience. All subjects felt a significant difference between the unactuated and actuated display, and characterized the latter as more "sticky" or "grabby".

During the second stage of the training session, the subjects became familiar with the range of stimuli to be presented in the experiment. They were given a freely adjustable "stickiness" knob on the touch screen. The knob value corresponded to the value of I_s and I_{ps} and ranged from 0 $\mathrm{mA_{pp}}$ to 8 $\mathrm{mA_{pp}}$. The subjects were given the opportunity to freely explore the effect for as long as they needed to become familiar with the range of experimental stimuli.

Eight stimuli were presented five times in a pseudo-random order. Each corresponded to a different current value from the range: $I_{out} = \{0, 2, 3, 4, 5, 6, 7, 8\}$ $\mathrm{mA_{pp}}$. No stimulus was rendered with 1 $\mathrm{mA_{pp}}$ because this provided minimally significant difference from base surface. Subjects were asked to rate the stimulus based on its apparent strength of "stickiness" using any scale of their choice. No feedback was given during the experiment. Free magnitude estimation responses were entered via the touchscreen into a MATLAB

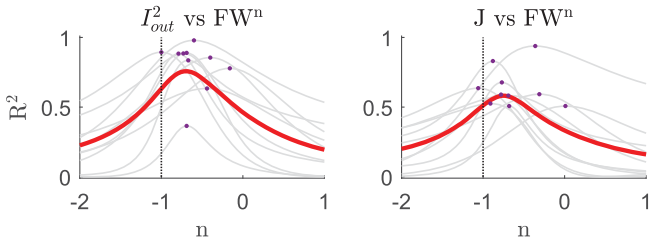

Fig. 5. Correlation strength between the square of applied electroadhesion current, I^2_{out}, and FW^n, as well as between stickiness judgment (J) and FW^n, as function of W exponent, n. Grey lines represent per-subject results, red represents the mean of R^2 values, and black vertical line corresponds to perfect stiction rendering. Black points correspond to curve peaks.

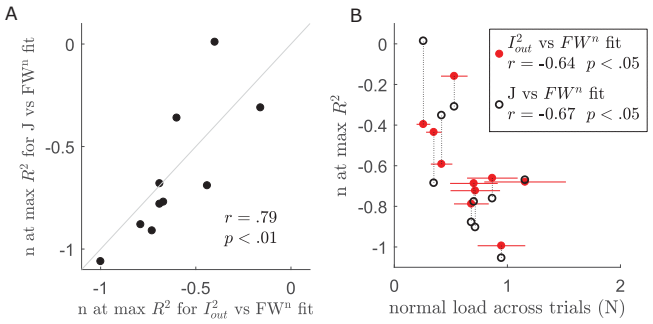

Fig. 6. A) Exponent n extracted from best judgment (J) vs FW^n and I^2_{out} vs. FW^n fits plotted against one another. Black line represents a one-to-one mapping. B) Exponent n extracted from the two fits plotted against mean normal load applied by the subjects. Horizontal lines represent standard deviation. Vertical lines connect results collected from the same subject.

GUI. The combined trial and experiment session lasted 15-20 minutes.

IV. Results

Figure 4 contains the free magnitude estimation results. There is a well-defined positive correlation between applied current and the perceived stickiness of each sample (r = .79, $\rho = .83$, $p < 10^{-10}$). with a 12-fold average increase in perceived stickiness from the base unactuated surface. Subjects performed 20.6 $\pm$ 13.4 ($mean \pm \sigma$) swipes and spent 5.8 $\pm$ 4.2 seconds per trial resulting in 3.8 $\pm$ 1.1 Hz (maximum 6.5 Hz) side to side motion of the finger. This somewhat high exploratory rate is not surprising since the perceptually rich effect was supplied only at the edges of a swipe and more frequent swipes produced more stimuli per unit time. The mean of judgment vs. current data in Figure 4 can be roughly fit by an attenuated power law function, similar to one observed between dynamic friction force and applied current for an experiment conducted on the same surface [15]. We use the square of the current value, I^2_{out}, as the parameter value that linearly adjusts surface stickiness for further analysis.

In order to narrow down which aspect of friction interaction was most robustly rendered by the device, we adopt a simplified friction model, $FW^n = k$, where the parameter k is controlled by current, and therefore, $k = k(I^2)$. If true stiction were to be rendered, then $n = -1$ and $FW^{-1} = \mu_s$, and therefore $\mu_s \propto I^2$. It is difficult to predict from given equations and the data at hand the value of this exponent for our case. For one, α during the estimated slip transition is not necessarily 0. In fact, there is evidence to the contrary [20], and it is possible that its value during slip transition is load and velocity dependent, as is the case for β [11]. Secondly, while under static load finger contact is well-approximated by a Hertzian model, it is unknown whether this holds true for a dynamic contact. Lastly, it has been empirically demonstrated that $\mu_s \propto W^{-2/3}$ [21], however, this model may fail in the presence of electroadhesion which itself is a function of contact area and therefore normal load. With these factors in mind, we performed a correlation-based analysis to find the predictive power of I^2_{out} on FW^n where F and W values were sampled at the instant of estimated transition from partial to full slip, allowing exponent n to vary (Figure 5 A). The results indicate the value of n which maximizes the goodness of fit between I^2_{out} and FW^n across all subjects is $n = -0.69$, with mean $R^2 = .76$ (p $< .0001$ at optimal R^2 across subjects), with exponent values varying significantly across subjects. This finding appears to be consistent with [21], suggesting that the mechanics of stiction have remained largely unchanged in the presence of electroadhesion. The true extent of this claim, however, needs further investigation.

Individual n values varied between -1, which corresponds to true stiction, and 0, which corresponds to lateral force rendering. We wished to assess the extent to which these deviations effected perception. We found that the judgment of surface stickiness was best predicted by FW^n where $n = -0.74$, with $R^2 = .56$ (p $< .0001$ for all subjects), which is very numerically close to the exponent we found from I^2 vs. FW^n fit (Figure 5 B). In fact, the exponent n which corresponded to the maximum correlation from the I^2_{out} vs. FW^n fit correlated to one from the judgment (J) vs. FW^n fit across our subjects (r = .79, $p < .01$) (Figure 6 A). It appears that the force interaction that was most robustly rendered by applied current was also the one upon which the stickiness judgment was made. In other words, the subjects utilized the most informative aspects of touch to base their judgment upon. It is unclear, however, whether the overall quality of rendering has deteriorated from the ideal rendering case, although it is unlikely likely that judgment performance has suffered as a consequence (r = -.07, p>.05 for correlation between variation in magnitude estimation and optimal exponent across subjects).

The predictive power of user-adjusted stickiness parameter, I^2_{out}, did not improve when linearly combined with the W term (ΔR^2 = 0, and ΔR^2 = .03 for current and judgment fits respectively). This suggests that the contribution of the normal load to perception of surface stickiness was negligible in comparison to the added effect of electroadhesion. The effect itself, however, was significantly impacted by the normal load, or more likely the contact area that is a function thereof (Figure 6 B). We found that best-fit exponent correlated with mean applied load (r = -.64, $p < .05$, and

r = -.64, $p < .05$, for current and judgment respectively) and subjects that applied larger normal loads on average experienced friction rendering closer to true stiction.

V. Discussion

Smooth-rough, soft-hard, and slippery-sticky are the three most salient dimensions which define a perceptual space of texture [22]. In current work we propose a novel method for rendering surface stickiness on a haptic surface by closed loop modulation of friction force. A psychophysical study was performed to 1) test the robustness of the stiction algorithm on an electroadhesion based device, and 2) elucidate the source of the perceptual quality associated with surface stickiness using a simplified fiction model. Our results indicate that the rendering model worked well in displaying a perceptual quality of "stickiness" for most subjects and functioned robustly to a variety of contact conditions such as a range of normal forces, velocities, and swipe directions. Although true stiction was not rendered for most subjects, this is unlikely to have affected the perception significantly as subjects tuned into the most informative aspect of touch to estimate the magnitude of the effect.

In this work we examined stickiness as the sole rendered feature on a surface haptic display. We anticipate that our rendering protocol can serve as an enhancement tool for more complex virtual tactile textures displayed on friction modulation displays. For example, it can be paired with texture rendering models that assume a fully dynamic state of the finger patch. In such scenarios, it is important to investigate whether perceptual salience of "stickiness" is unperturbed when texture features are added. For instance, it is not clear whether the exploratory procedures for stickiness perception (i.e., frequent reversals) would be maintained in the presence of additional textural richness. In addition, there may be other sources of stickiness information that arise in dynamic movements across complex textures.

VI. Acknowledgements

This work was supported by the National Science Foundation grant number IIS-1518602. The authors would like to thank Prof. Roberta Klatzky for many productive discussions.

References

[1] Yitian Shao, Vincent Hayward, and Yon Visell. Spatial patterns of cutaneous vibration during whole-hand haptic interactions. *Proceedings of the National Academy of Sciences*, 113(15):4188–4193, 2016.

[2] RS Johansson and JR Flanagan. Tactile sensory control of object manipulation in humans. *The Senses: A Comprehensive Reference, Academic Press, New York, NY*, pages 67–86, 2008.

[3] Roland S Johansson and J Randall Flanagan. Coding and use of tactile signals from the fingertips in object manipulation tasks. *Nature Reviews Neuroscience*, 10(5):345, 2009.

[4] RS Johansson and G Westling. Roles of glabrous skin receptors and sensorimotor memory in automatic control of precision grip when lifting rougher or more slippery objects. *Experimental brain research*, 56(3):550–564, 1984.

[5] Shogo Okamoto, Michael Wiertlewski, and Vincent Hayward. Anticipatory vibrotactile cueing facilitates grip force adjustment during perturbative loading. *IEEE transactions on haptics*, 9(2):233–242, 2016.

[6] R. V. Grigorii, M. A. Peshkin, and J. E. Colgate. High-bandwidth tribometry as a means of recording natural textures. In *2017 IEEE World Haptics Conference (WHC)*, pages 629–634, June 2017.

[7] Louise R Manfredi, Hannes P Saal, Kyler J Brown, Mark C Zielinski, John F Dammann III, Vicky S Polashock, and Sliman J Bensmaia. Natural scenes in tactile texture. *Journal of neurophysiology*, 111(9):1792–1802, 2014.

[8] Sliman Bensmaïa, Mark Hollins, and Jeffrey Yau. Vibrotactile intensity and frequency information in the pacinian system: A psychophysical model. *Perception & psychophysics*, 67(5):828–841, 2005.

[9] Anne-Sophie Augurelle, Allan M Smith, Thierry Lejeune, and Jean-Louis Thonnard. Importance of cutaneous feedback in maintaining a secure grip during manipulation of hand-held objects. *Journal of Neurophysiology*, 89(2):665–671, 2003.

[10] Thibaut André, V Lévesque, V Hayward, Philippe Lefèvre, and J-L Thonnard. Effect of skin hydration on the dynamics of fingertip gripping contact. *Journal of The Royal Society Interface*, 8(64):1574–1583, 2011.

[11] Benoit Delhaye, Philippe Lefevre, and Jean-Louis Thonnard. Dynamics of fingertip contact during the onset of tangential slip. *Journal of The Royal Society Interface*, 11(100):20140698, 2014.

[12] David Gueorguiev, Séréna Bochereau, André Mouraux, Vincent Hayward, and Jean-Louis Thonnard. Touch uses frictional cues to discriminate flat materials. *Scientific reports*, 6:25553, 2016.

[13] Subrahmanyam M Pasumarty, Simon A Johnson, Simon A Watson, and Michael J Adams. Friction of the human finger pad: influence of moisture, occlusion and velocity. *Tribology Letters*, 44(2):117, 2011.

[14] Mélisande Biet, Frédéric Giraud, and Betty Lemaire-Semail. Squeeze film effect for the design of an ultrasonic tactile plate. *IEEE transactions on ultrasonics, Ferroelectrics and Frequency control*, 54(12):2678–2688, 2007.

[15] Craig Shultz, Edward Colgate, and Michael A Peshkin. The application of tactile, audible, and ultrasonic forces to human fingertips using broadband electroadhesion. *IEEE Transactions on Haptics*, 2018.

[16] Craig D Shultz, Michael A Peshkin, and J Edward Colgate. Surface haptics via electroadhesion: Expanding electrovibration with johnsen and rahbek. In *World Haptics Conference (WHC), 2015 IEEE*, pages 57–62. IEEE, 2015.

[17] F. Giraud, M. Amberg, and B. Lemaire-Semail. Merging two tactile stimulation principles: electrovibration and squeeze film effect. In *2013 World Haptics Conference (WHC)*, pages 199–203, April 2013.

[18] Craig D. Shultz, Michael A. Peshkin, and J. Edward Colgate. On the electrical characterization of electroadhesive displays and the prominent interfacial gap impedance associated with sliding fingertips. *2018 IEEE Haptics Symposium (HAPTICS)*, pages 151–157, 2018.

[19] Vincent Hayward and Brian Armstrong. A new computational model of friction applied to haptic rendering. In *Experimental Robotics VI*, pages 403–412. Springer, 2000.

[20] Alexander V Terekhov and Vincent Hayward. Minimal adhesion surface area in tangentially loaded digital contacts. *Journal of biomechanics*, 44(13):2508–2510, 2011.

[21] Hyun-Yong Han, Akihiro Shimada, and Sadao Kawamura. Analysis of friction on human fingers and design of artificial fingers. In *Robotics and Automation, 1996. Proceedings., 1996 IEEE International Conference on*, volume 4, pages 3061–3066. IEEE, 1996.

[22] Mark Hollins, Richard A. Faldowski, Sujata Rao, and F Young. Perceptual dimensions of tactile surface texture: a multidimensional scaling analysis. *Perception psychophysics*, 54 6:697–705, 1993.